frontiers in Materials

REVIEW
published: 24 May 2021
doi: 10.3389/fmats.2021.674798

Designing Oxide Aerogels With Enhanced Sorptive and Degradative Activity for Acute Chemical Threats

Travis G. Novak[1], *Paul A. DeSario*[2]*, *Jeffrey W. Long*[2] *and Debra R. Rolison*[2]

[1]National Research Council Postdoctoral Associate, US Naval Research Laboratory, Washington, DC, United States, [2]US Naval Research Laboratory, Surface Chemistry Branch, Washington, DC, United States

Oxide aerogels are pore–solid networks notable for their low density, large pore volume, and high surface area. This three-dimensional arrangement of pore and solid provides critical properties: the high surface area required to maximize the number of active sites and a through-connected porosity that plumbs reactants to the active interior. In decontamination applications where reactivity beyond adsorption is desired to degrade deleterious molecules, oxide aerogels offer multiple avenues to add oxidative power to this unique arrangement of pore and solid. For protection against chemical warfare agents or toxic industrial chemicals, metal-oxide aerogels with their oxide/hydroxide surfaces afford stability under ambient conditions against competing sorbents such as water and oxygen. In this review, strategies to maximize sorptive capacity and degradation rate by modifying surface functionality, compositing with dissimilar oxides, or adding metallic nanoparticles and the subsequent impact on decontamination performance will be summarized and expected directions for future research will be discussed based on the observed trends.

Keywords: aerogel, decontamination, chemical warfare agent, metal oxide, catalyst, toxic industrial chemical

OPEN ACCESS

Edited by:
Xuetong Zhang,
Suzhou Institute of Nano-Tech and Nano-Bionics (CAS), China

Reviewed by:
Wei Wei,
Jiangsu University, China
Junzong Feng,
National University of Defense Technology, China
Ran Du,
The University of Hong Kong, China

***Correspondence:**
Paul A. DeSario
paul.desario@nrl.navy.mil

Specialty section:
This article was submitted to Polymeric and Composite Materials, a section of the journal Frontiers in Materials

Received: *02 March 2021*
Accepted: *29 April 2021*
Published: *24 May 2021*

Citation:
Novak TG, DeSario PA, Long JW and Rolison DR (2021) Designing Oxide Aerogels With Enhanced Sorptive and Degradative Activity for Acute Chemical Threats. Front. Mater. 8:674798. doi: 10.3389/fmats.2021.674798

INTRODUCTION: THE CHALLENGE OF MATERIALS DESIGN FOR MITIGATION OF HAZARDOUS MOLECULES

All technology has unintended consequences, occasionally beneficial, too often detrimental (Tenner, 1997). Chemistry brings people the wonders of modern life, but when chemical technology is not informed by a lifecycle analysis of the fate of chemicals, environmental quality can be compromised. A chronic problem can then arise from environmental accumulation of chemical species deleterious to lifeforms (not just humans), counterbalanced by new materials and processes developed to sequester those chemical species. This type of environmental remediation can be viewed as ameliorating long-term exposure and inform such actions as removing heavy metal ions from water, preventing oil spills from infiltrating the food chain, photocatalyzing decomposition of organic offshoots of the chemical industry, or sequestering CO_2. Another class of chemical species, however, poses an acute risk, such as the threats posed by chemical warfare (CW) agents and toxic industrial chemicals (TICs).

Materials that neutralize CW agents and TICs find applicability in both the military and civilian realms, from deliberate release of chemical agents as a hostile act to industrial accidents (Smith, 2008; DeCoste and Peterson, 2014; Mukhopadhyay et al., 2020). Common CW agents, CW simulants, and TICs are inhalation and contact hazards; selected molecular structures for these classes are shown in **Figure 1**. At present, personal protection from toxic vapors relies almost exclusively on activated carbons, but there is vast room for improvement over these traditional materials. Activated carbon

acts solely as an adsorbent material with the caveat that it does not effectively adsorb molecules with high vapor pressures. Those toxic chemicals that do adsorb persist intact such that the spent materials pose the threat of re-exposure, additionally becoming a disposal burden. Activated carbons are impregnated with acids, amines, and certain metals to incorporate additional acid/base chemistry for reaction with higher-volatility compounds. However, even impregnated carbons do not fully neutralize toxic chemicals and may suffer from poor shelf-stability (DeCoste and Peterson, 2014). Other types of highly porous carbon, referred to as aerogels due to their mesoporosity and foam-like morphology, are derived from pyrolyzed polymer foams or freeze-dried foams containing graphene (Lee and Park, 2020) and function similarly to activated carbon, adsorbing intact CW agents (Han et al., 2017) and environmental pollutants (Gan et al., 2019).

For superior protection, multifunctional mitigation materials are desired that rapidly adsorb and degrade chemical threats into nontoxic products, thus negating the risk of re-exposure and easing the disposal burden of spent materials. Although reactive degradation is far preferred over adsorption, better still are materials that allow regeneration (turnover) of reactive/adsorptive sites such that the material remains active for prolonged lifetimes and/or multiple usage cycles. Beyond these functional requirements, DeCoste and Peterson recently highlight design considerations for formulating new, higher performance materials. Namely, reactive sorbents should operate under a full range of ambient temperature and humidity conditions, and retain functionality after the processing required to formulate into physically stable engineered forms. They note that materials must effectively provide protection while doing so practically, i.e., "balancing weight, volume, hardness, and resistance to aging" (DeCoste and Peterson, 2014).

In decontamination applications where reactivity beyond adsorption is desired, oxide aerogels provide: 1) a high surface area required to maximize the number of active sites, 2) a through-connected porosity that plumbs reactants to the active surface, and 3) multiple avenues to add oxidative power to this unique arrangement of pore and solid. Aerogels—a broad class of materials derived from wet gels dried in a manner that limits collapse of pore structure—are solid monolithic structures notable for their low density, large pore volume, high surface area, and continuous meso/macro/micro pore networks (Kistler, 1931; Pierre and Pajonk, 2002). Aerogels were first synthesized in 1931 (Kistler, 1931), but attracted more extensive research interest in later decades with developments in synthesis, notably the introduction of simplified sol–gel methods using alkoxide precursors in the 1960s and supercritical CO_2 drying of the wet gel in the 1980s (Pajonk, 1994). Aerogels have been constructed from oxides (Rolison et al., 2020), carbon (Gan et al., 2019), chalcogenides (Mohanan et al., 2005), metals (Wang et al., 2020), cellulose (Wang et al., 2017b), nitrides (Wang et al., 2019), and MXenes (Zhang et al., 2020) among other materials. Due to their low density, aerogels are commonly utilized as thermal insulators, and their combination of high-surface area and mesoporosity makes them appealing for use as adsorptive materials, heterogeneous catalysts, and for electrochemical charge storage (Pierre and Pajonk, 2002).

Because of their desirable structural properties, aerogels of a wide range of chemical compositions (carbon, chalcogens, cellulose, etc.) have been developed as high-performance sorbents in various environmental remediation and filtration applications, including removal of heavy metal ions, degradation of organic dyes, oil-spill cleanup, adsorption of hydrocarbons, and CO_2 capture (Ahmed et al., 2014; Gan et al., 2019; Hasanpour and Hatami, 2020; Maleki, 2016; Wang et al., 2017b). The base compositions of aerogels are also readily functionalized with other chemical moieties, either during the synthesis/processing steps or post-synthesis modification, to yield multifunctional aerogels that are tuned for specific applications (Long and Rolison, 2007). For protection against chemical warfare agents or toxic industrial chemicals, metal-oxide aerogels with their oxide/hydroxide surfaces, serve as reactive adsorbents with demonstated high performance for a wide variety of CW agents and TICs (**Table 1**) and afford stability under ambient conditions against competing sorbents such as water and oxygen. Nanostructured metal oxides and hydroxides, such as aerogels, neutralize chemical threats because they possess physisorptive, chemisorptive, and/or catalytically active surface sites. Nanocrystalline oxides drive CW agent and TIC degradation by various mechanisms, such as oxidation, hydrolysis, elimination, and dealkylation (Tang et al., 2008; Saxena et al., 2009).

Other classes of high-surface area, mesoporous materials have also been investigated for use as protective materials from acute chemical threats, including MOFs, zeolites, and molecular sieves, but all of these materials suffer from limitations. Metal–organic

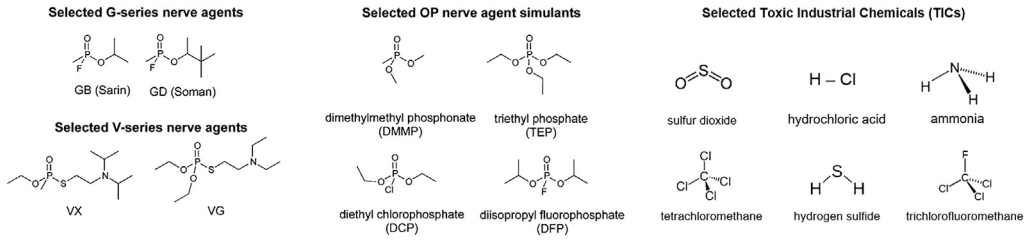

FIGURE 1 | Molecular structure of common CW agents, CW simulants, and TICs. Adapted from Dennison et al. (2014) with permission from the Royal Society of Chemistry.

TABLE 1 | Summary of key oxide aerogel compositions and the reactions evaluated.

Material	Reaction	Reference
Single Oxides		
CaO	CCl_4	Koper et al. (1993)
MgO	Pyridine, benzene, xylene, nitrobenzene	Itoh et al. (1993)
ZrO_xH_y	DMMP	Long et al. (2020)
MgO	VX, GD, HD, 2-CEES	Wagner et al. (1999)
CaO	VX, GD, HD, 2-CEES	Wagner et al. (2000)
Al_2O_3	VX, GD, GB, HD	Wagner et al. (2001)
MgO, Al_2O_3, CaO, SiO_2	DEClP	Saxena et al. (2010a)
MgO	1-Chlorobutane	Shuvarakova et al. (2018)
MnO*x*	NH_3, H_2S, SO_2	Long et al. (2016)
Al_2O_3 impregnated with MoVPA, PTA, NaOH or K_2OsO_4	2-CEES, DECIP	Saxena et al. (2009);Saxena et al. (2010b)
Composites		
CaO or MgO coated with Fe_2O_3, NiO, or CoO	SO_2, CO_2, HCl, CCl_4	Klabunde et al. (1996)
Core-shell (Fe_2O_3)MgO, (Fe_2O=)Cao, (V_2O_3)MgO	CCl_4, $CHCl{=}CCl_2$, $C_6H_4Cl_2$, DMMP	Jiang et al. (1998)
Core–shell (Fe_2O_3)MgO, (Fe_2O_3)CaO	H_2S	Carnes et al. (2002)
Core–shell (V_2O_3)MgO	CCl_3F	Martyanov and Klabunde (2004)
Co-gelled Al_2O_3/MgO	CCl_4, SO_2, Paraoxon	Carnes et al. (2002)
Al_2O_3 co-gelled with Fe_2O_3, V_2O_5, or CuO	HD	Prasad et al. (2010)
Fe_2O_3 or SiO_2 particles added to MgO precursors	2-CEES	Vu et al. (2015)
Au or Cu nanoparticles on TiO_2 aerogels	DMMP, GB	DeSario et al. (2021); McEntee et al. (2020)

frameworks (MOFs) are intriguing materials for hazardous compound decontamination because they possess high surface areas (up to 1,000s of m^2g^{-1} as measured by small-molecule physisorption) and tailorable functional groups (Cavka et al., 2008; Khan et al., 2013; DeCoste and Peterson, 2014; DeCoste et al., 2015; Mondloch et al., 2015; Islamoglu et al., 2020). However, many MOFs have modest chemical, thermal, and mechanical stability and are unstable in water (Canivet et al., 2014; DeCoste and Peterson, 2014). Among MOFs that are well suited to toxic-gas filtration, many of them undergo structural rearrangements and an order-of-magnitude decline in surface area upon exposure to water. Modifications to render MOFs more water-stable, such as exchanging organic linkers or varying the metal center, may come at the expense of filtration performance (DeCoste and Peterson, 2014; Son et al., 2020; Song et al., 2020). **Figure 2** highlights the stark contrast in uptake of selected MOFs under dry (0% RH) vs. humid (80% RH) conditions (Chen et al., 2020). Furthermore, during CW agent hydrolysis certain Zr-based MOFs form tightly bound products that render them ineffective as gas-phase catalysts (Wang et al., 2017a).

Despite their high surface area, the small pore aperture of most MOFS means that interactions with larger molecules occur at the crystallite surface rather than within the MOF pores (Mondloch et al., 2015; Wang et al., 2017a). A high surface area implies a high number of reactive sites, but these active sites are wasted if the vapor phase must access them through micropores (defined as <2 nm). Practical performance requires a hierarchical pore network, with micropores connected to mesopores (2–50 nm) and even small macropores (>50 nm), such that molecular diffusion can approach open-medium rates while still maintaining contact to a high number density of active sites.

Crystalline porous oxides known as zeolites are water- and thermally stable minerals known since the 18th century (Schwochow and Puppe, 1975; Davis and Lobo, 1992). Microporous networks defined synthetically in one, two, or three dimensions allow size- and shape-controlled sorption of organics into the high surface–area interior. Zeolites can be chemically modified with nanoparticles or inorganic coordination complexes or ion exchanged with more chemically reactive cations that replace the alkali or alkaline earth cations present in the native zeolite that charge balance Al^{3+} in the oxide framework. Zeolites enable valuable technologies from ion exchange (such as water softening or remediation of radioactive Cs^+ from aqueous waste) to separations (even distinguishing *ortho*, *meta*, *para* aromatics) to adsorption to catalysis (such as fluid catalytic cracking to

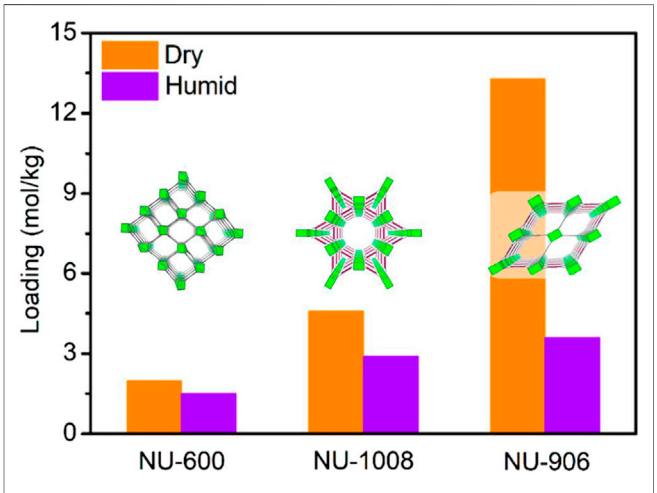

FIGURE 2 | 2-chloroethyl ethylsulfide (2-CEES) loading of three zirconium-based MOFs under dry (0% RH) and humid (80% RH) conditions. Adapted from Chen et al. (2020) with permission from the American Chemical Society.

produce high-octane gasoline), but they can also adsorb and potentially detoxify simulants and CW agents (Yekta et al., 2019). But just as with MOFs, microporous entrances and exits into the high surface area of the zeolite's interior compromise rate-critical applications (Rolison, 2003) such as CW agent or TIC mitigation where the number of molecules affected per second matters. Similarly, silica-based molecular sieves can adsorb CW agents, but suffer from slow kinetics compared to traditional activated carbon (Meneses et al., 2008).

Although some MOFs and zeolites may exhibit moderately higher surface area and pore volume than oxide aerogels, the predominance of 3D-plumbed mesoporosity in the latter ensures that all surface area is accessible to molecules and ions. The combination of facile mass transport, ability to incorporate adsorptive and degradative activity, and their stability under practical conditions make oxide aerogels an especially promising class of materials for advanced degradation applications. In the following sections, we discuss the advantages accrued by expressing metal oxides as aerogel and aerogel-like pore–solid architectures over traditional oxide materials in the context of eliminating threats posed by CW agents and TICs. We review ways in which oxide aerogels have been physically or chemically modified to increase applicability, including how defect site or surface OH group density is increased to enhance chemical degradation. We highlight more recent work on the design of aerogel-based composites—including mixed oxides or metal nanoparticle–decorated oxides—that incorporate multiple functions to enhance performance for decontamination of hazardous compounds. We also discuss how different degradation pathways can be activated using semiconducting oxides or plasmonic nanoparticles.

EFFECT OF COMPOSITION AND MORPHOLOGY FOR STOICHIOMETRIC OXIDE AEROGELS

A basic illustration of sol–gel synthesis of oxide aerogels is shown in **Figure 3**. While many variations of these methods exist, the most common route includes hydrolysis of the precursor, replacing alkoxide groups (–OR) with hydroxide groups (–OH), followed by condensation of –OH-terminated species to form M–O–M bonds. Further growth through hydrolysis and crosslinking results in a continuous, aperiodic network within the liquid phase (Rechberger and Niederberger, 2017). Because capillary forces established during evaporative drying under ambient conditions compress the nanometric pore walls and risk condensing interfacial M–OH on opposite walls thereby reducing free volume, supercritical drying minimizes surface tension such that pressure release effectively replaces the liquid phase with air while still preserving the gel structure.

High surface–area oxides can also be synthesized through various template-based nanopatterning techniques. For electrocatalysts and photocatalysts, nanosphere lithography (Lee et al., 2017; Brinkert et al., 2018), nanoimprint lithography (Contreras et al., 2006; Xie et al., 2019), proximity-field nanopatterning (Ahn et al., 2013; Kim et al., 2019; Tiwari et al., 2020), and other similar methods (Xu et al., 2020) are widely explored to create highly porous, periodic structures that more effectively expose active sites than occurs with MOFs or zeolites. However, these template-based approaches are typically applicable only to thin films supported on substrates, making them unsuitable for TIC/CW agent remediation where a large quantity of the freestanding material must be economically synthesized. Our review thus focuses on the more manufacturable sol–gel-derived oxide aerogels.

In their pioneering work, Klabunde and co-workers established the efficacy of sol–gel-derived alkaline-earth and transition metal–oxide aerogels as reactive adsorbents for TICs and CW agents. Recognizing that destruction of toxic chemicals is accomplished mainly through noncatalytic surface reactions that are thermodynamically favorable on most oxide surfaces, they focused on preparation of high surface–area oxides. They initially explored aerogel preparations of CaO and MgO, and later evaluated aerogel-prepared (AP) Al_2O_3, ZnO, V_2O_5, TiO_2, and SiO_2 (**Table 1**). Their findings consistently show that aerogel preparations of oxides outperform conventionally prepared (CP) counterparts, even when nanometric, for removal of a variety of compounds, including chlorocarbons, organophosphorous compounds, acid gases, and nerve agents.

The enhanced surface area and facilitated mass transport characteristic of solids expressed as co-continuous pore–solid architectures account for much of the improved performance of

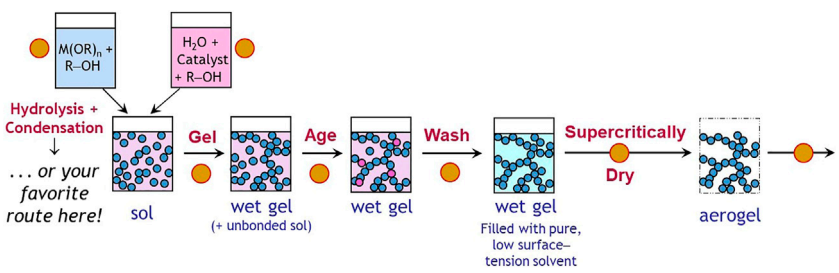

FIGURE 3 | Illustration of the sol–gel synthetic route to aerogels, including the many points (●) during the synthetic and processing steps at which new physicochemical functionality can be introduced.

aerogels, but in many cases, aerogels outperform CP oxides even when normalizing to specific surface area (SA). Expressing an oxide as an aerogel also leads to changes in intrinsic surface chemistry of the oxides (Koper et al., 1997). The nanoscale oxide particles characteristic of aerogels facilitate a high number of edge and corner defect sites and may stabilize lattice planes that would be minimally expressed in larger particles (Wagner et al., 2000), in agreement with the thermodynamics of nanometric oxides established using calorimetry (Navrotsky, 2011). The acidity/basicity of oxide surfaces also depends on SA/particle diameter. Small particles characteristic of the aerogel preparation possess a higher ratio of edge:surface sites, and thereby favor monodentate binding vs. particles with wider faces that favor bidentate bonding. The aerogel-prepared materials also possess persistent, isolated OH groups, even at high temperatures in vacuum conditions (Koper et al., 1997). A final benefit of an aerogel route to high surface-area oxides lies in the fact that the oxide nanoparticles generate a covalently networked solid, which prevents particulate agglomeration and consequent occluded mesoporous volume typical of nanoscale powders.

Over a range of reactions probing the activity of CP-CaO and CP-MgO versus their AP versions for molecular degradation (**Table 1**), the Klabunde group validates that both surface area and intrinsic surface activity dictate mitigation efficacy. Small nanocrystallites of AP-MgO and AP-CaO contain more edge sites, four-fold under-coordination sites, and oxygen (O^{2-}) vacancies compared to CP-MgO and CP-CaO (Itoh et al., 1993; Klabunde et al., 1996). Both the basicity and distribution of surface–OH groups on aerogel surfaces determine the performance of MgO and CaO aerogels for removal of SO_2, CO_2, HCl, CCl_4, and the organophosphorus CW simulant, dimethyl methylphosphonate (DMMP) (Klabunde et al., 1996). The elution of DMMP through AP vs. CP-MgO and CaO clearly shows the superior destructive adsorption capacity of the AP oxides as enhanced by their greater basicity (**Figure 4A**). Isolated–OH groups favor monodentate rather than bidentate binding, of importance for enhancing the uptake of SO_2 and CO_2 on the AP oxides (Klabunde et al., 1996; Koper et al., 1997).

The choice of oxide must account for its surface reactivity, not just its ability to be expressed as a high surface area, mesoporous aerogel. A comparison of various oxide aerogels for removal of H_2S highlights that both kinetics and thermodynamics are important (Carnes and Klabunde, 2002). For CaO, MgO, Al_2O_3, and ZnO aerogels, kinetics factors dominate because higher degradation efficiencies result when using smaller crystallites with higher surface areas. But for oxides where the surface reaction with H_2S is thermodynamically unfavorable (MgO and Al_2O_3), some H_2S is degraded, but full surface reactions are not obtained. In contrast, a stoichiometric reaction is realized for oxides where the H_2S surface reaction is thermodynamically favored (ZnO and CaO). For CaO in particular, the reaction proceeds into the "bulk" of the nanocrystals, which is attributed to edge/corner or defect sites that facilitate H_2S penetration (Carnes and Klabunde, 2002).

Aerogel-prepared CaO (Wagner et al., 2000), MgO (Wagner et al., 1999), and Al_2O_3 (Wagner et al., 2001) were subsequently tested for removal of CW agents soman, nerve agent (VX), and mustard gas (HD), as well as the CW simulant 2-chloroethyl ethylsulfide (2-CEES). All three aerogels stoichiometrically degrade soman and VX by hydrolytic pathways whereas HD degrades by both hydrolysis and HCl elimination pathways (Wagner et al., 1999; Wagner et al., 2000; Wagner et al., 2001). For reaction of soman and VX at CaO and MgO, two kinetics regimes occur. A fast, initial rate of removal is attributed to facile liquid-phase mass transport of the CW agent through the aerogel pores while reactive adsorption occurs at the wave front. The fast reaction terminates once liquid spreading ceases. At that point, the steady-state first-order reaction rate is mediated by evaporation rate and depends on the vapor pressure of the CW agent; gas-phase diffusion is not rate-limiting (Wagner et al., 1999; Wagner et al., 2000). **Figure 4B** shows the distinct fast and slow kinetics regimes for VX degradation over MgO aerogels. For Al_2O_3, only VX follows two kinetics regimes.

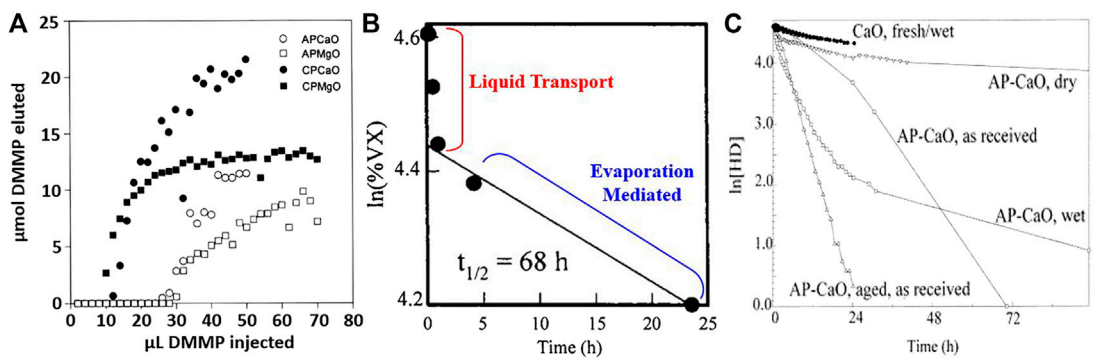

FIGURE 4 | (A) Comparison of destructive adsorption of DMMP over aerogel-prepared (AP) and conventionally prepared (CP) nanometric oxides. Adapted from Klabunde et al. (1996) with permission from the American Chemical Society. **(B)** Reaction profile of VX on AP-MgO. Adapted from Wagner et al. (1999) with permission from the American Chemical Society. **(C)** Reaction profile for HD on CaO and AP-CaO under various conditions. Adapted from Wagner et al. (2001) with permission from the American Chemical Society.

For HD, degradation occurs via hydrolytic and HCl elimination pathways to varying extents that depend upon oxide composition and reaction conditions. The percentage of total HD degraded by HCl elimination was 17%, 50%, and 80% for Al_2O_3, MgO, and CaO, respectively (Wagner et al., 1999; Wagner et al., 2001; Mukhopadhyay et al., 2020). Like VX and soman, HD degradation has an initial fast reaction followed by a slower, steady-state reaction on all oxides. The only exception is HD reaction on partially hydrated CaO aerogel, which occurs by fast steady-state elimination of HCl after an induction period. The induction period is attributed to conversion of a surface layer of CaO to $CaCl_2$, which is a more active dehydrohalogenation catalyst than CaO. The rapid reaction that follows necessitates surface water to drive acid-catalyzed surface reconstruction, which continually replenishes the surface. Heavily hydrated CaO aerogel does not show the same rapid autocatalytic behavior, suggesting that too much adsorbed water prevents HD from binding to the oxide surface (**Figure 4C**) (Wagner et al., 2000).

Similar reactivity occurs at MgO aerogels for dehydrochlorination of 1-chlorobutane adsorbed from the gas phase with a substantial increase in catalytic activity as MgO partially converts to $MgCl_2$ (Shuvarakova et al., 2018). The authors use perylene as a molecular probe to reveal the presence of electron-acceptor sites on the MgO surface during reaction with 1-chlorobutane. They report that the MgO aerogel surfaces initially do not contain the electron-acceptor sites needed to drive acid-catalyzed reactions (ex., 1-chlorobutane degradation or HD degradation). The electron-acceptor sites appear during dehydrochlorination as MgO reacts with the generated Cl^-. They conclude that these sites are Brønsted acid sites resembling chemisorbed HCl fragments on the MgO surface (Shuvarakova et al., 2018).

In a study of various classes of porous sorbents, Winter et al. compared the performance vs. carbon of a series of metal oxides with wide-ranging surface areas (10s of m^2g^{-1} to >1000 m^2g^{-1}) and pore volumes (10^{-2} to >1 cm^3g^{-1}) (Winter et al., 2009). Although aerogels were not included in this study, the mesoporous oxides they evaluate have surface areas comparably high to aerogels. In order to down-select materials that offer broad applicability, they compare adsorption of SO_2 and the CW simulant 2-CEES: the former is volatile and polar while the latter relatively nonvolatile and nonpolar. Their work affirms that carbon works well only for nonvolatile and nonpolar materials, whereas, among all the oxides tested, TiO_2 and MgO show the best dual performance for both compounds (**Figure 5**). By comparing compositionally similar but structurally different porous solids, they confirm that high surface area and pore volume are crucial elements dictating reactive adsorption, but once adequate surface area and porosity are present, degradation rates are then dictated by the chemical properties of the surface. Polar oxide surfaces that provide isolated –OH sites and Lewis base/Lewis acid sites are the best at not only adsorbing, but also degrading, polar and nonpolar compounds (Winter et al., 2009).

Saxena et al. also report a side-by-side comparison of multiple oxides (MgO, Al_2O_3, CaO, and SiO_2), but expressed as aerogels, and conclude that MgO outperforms the other oxides for removal of the nerve agent simulant diethyl chlorophosphate (DCP, **Figure 1**). The MgO aerogels have the fastest adsorption kinetics and the highest adsorption capacity for DCP among the oxides tested, although CaO has higher adsorption capacity normalized to specific surface area (Saxena et al., 2010a). Their activity trend agrees with the above study in which MgO outperforms Al_2O_3 for removal of another nerve agent simulant, 2-CEES (Winter et al., 2009).

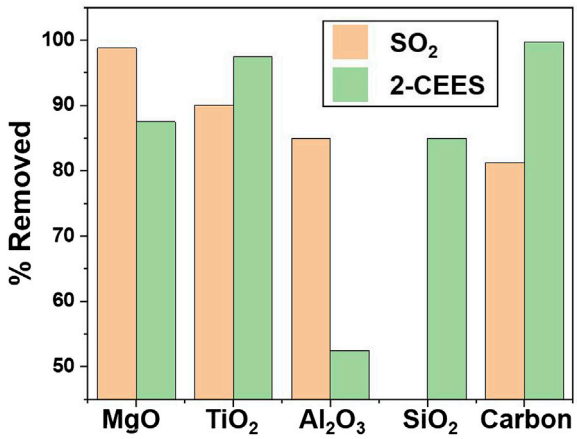

FIGURE 5 | Comparison of various high surface area oxides and carbon for adsorption of SO_2 and 2-CEES, data adapted from Winter et al. (2009).

OPTIMIZATION OF OXIDE/HYDROXIDE PHASES IN ZIRCONIUM- AND MANGANESE-BASED AEROGELS

While the previous section explored early work with largely stoichiometric oxide aerogels, transition metals such as Zr and Mn offer options to explore more complex non-stoichiometric oxides and hydroxide phases. The family of manganese oxides (MnO*x*) exhibits a rich diversity of crystal structures, defect structures, and substituted compositions that can be tuned for a variety of applications, including as sorbents and catalysts for such toxic compounds as formaldehyde, ozone, 2-CEES, and carbon monoxide (Prasad et al., 2007; Wang et al., 2015; Dey and Praveen Kumar, 2020; Zhang et al., 2021). Expressing MnO*x* in an aerogel-like morphology offers the opportunity to combine the surface area and mass-transport advantages inherent to aerogel architectures with the sorption/catalytic functionality of particular MnO*x* polymorphs and compositions (Long et al., 2016). For example, Long et al. synthesized MnO*x* aerogels by oxidizing fumaric acid with aqueous permanganate to form gels (Livage and Sanchez, 1992), which they then supercritically dried. This process generates low-density mesoporous monoliths in which the walls of the pore–solid architecture comprise networked nanolaths of birnessite-type MnO*x*, a layered polymorph (**Figures 6A,B**). Denser xerogel counterparts are also prepared from the same wet gel by drying at ambient pressure. Powdered forms of these MnO*x* aerogels and

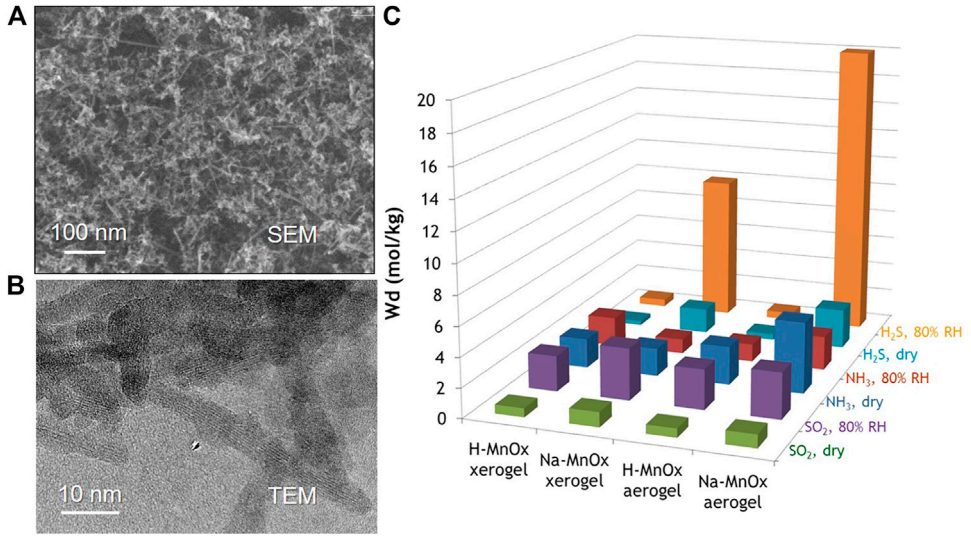

FIGURE 6 | (A) SEM and **(B)** TEM of MnO*x* aerogels. Adapted from Long et al. (2016) with permission from the American Chemical Society. **(C)** Comparison of H_2S, NH_3, and SO_2 uptake under dry and humid conditions.

xerogels were tested by microbreakthrough techniques for their filtration efficacy against common TICs including NH_3, SO_2, and H_2S (**Figure 6C**) (Long et al., 2001).

Under dynamic-challenge conditions with NH_3 (2,000 mg m^{-3} in balance of air), beds of MnO*x* aerogel powder exhibit sorption/capture capacity as high as 4.8 mol kg^{-1} (82 mg g^{-1}) in dry flow conditions. The MnO*x* xerogels also uptake NH_3 in breakthrough tests but at lower specific capacity (1–2 mol kg^{-1}), confirming that the larger pores (10–80 nm) and greater cumulative pore volume (~2.0 cm^3g^{-1}) of the aerogel form are beneficial for filtration under dynamic-flow conditions. The high NH_3 capacity of the MnO*x* aerogel is competitive with values reported for common MOFs examined under similar breakthrough testing, despite the MnO*x* aerogels having significantly lower specific surface area (~250 m^2g^{-1}) compared to MOFs (typically >1,000 m^2 g^{-1}) (Peterson et al., 2014; Jasuja et al., 2015). The MnO*x* aerogel also retains a relatively high NH_3 capacity of 2.3 mol kg^{-1} when the NH_3 feed stream is mixed with H_2O vapor to 80% relative humidity, a critical performance characteristic for practical filtration applications. For both aerogel and xerogel MnO*x*, capture is facilitated in part by intercalation of NH_3 between the layers of the birnessite structure, as previously shown for non-aerogel birnessite-type MnO*x* (Wang and Kanoh, 2001). In the case of these MnO*x* nanoarchitectures, the walls of the networked solid have built-in sites for the specific capture/sieving of NH_3, which readily diffuses to these active sites via the through-connected pore network.

In addition to capture mechanisms, manganese oxides serve as redox-active substrates in which $Mn^{3+/4+}$ reactions mediate the oxidation or reduction of molecules that adsorb at their surface. For example, MnO*x* aerogels exhibit SO_2-uptake capacities as high as 1.0 mol kg^{-1} (64 mg g^{-1}) under dry conditions and 3.5 mol kg^{-1} (220 mg g^{-1}) at 80% RH in microbreakthrough testing; these values are competitive with many MOF compositions of higher specific surface area (Martínez-Ahumada et al., 2020). Removal of SO_2 is achieved by its well-known oxidation to SO_4^{2-} on MnO*x* surfaces (Li et al., 1968; Vadjić and Gentilizza, 1985; Qu et al., 2013). Hydrogen sulfide also reacts specifically with MnO*x* aerogels and xerogels, but through a different mechanism in which polysulfides are formed on the oxide surface concomitant with reduction of the mixed-valent ($Mn^{3+/4+}$) oxide to MnOOH. Removal capacities for H_2S at MnO*x* aerogels reach 1.7 mol kg^{-1} (58 mg g^{-1}) under dry conditions, while the presence of co-adsorbed water under 80% RH increases the H_2S removal capacity to an impressive 20 mol kg^{-1} (680 mg g^{-1}). The ability of MnO*x* aerogels to effectively remove three chemically distinct TICs—NH_3, SO_2, and H_2S—at technologically relevant capacities under humid, not just dry conditions, makes these materials promising candidates for further development as air-filtration media.

Over the past decade, zirconium hydroxides have emerged as a leading contender for filtration of common TICs such as Cl_2 (Peterson and Rossin, 2012) and SO_2 (Peterson et al., 2009), and reactive decontamination of multiple categories of CW agents and simulants (Bandosz et al., 2012). Inspired by these advances with conventional $Zr(OH)_4$, we recently explored zirconium oxyhydroxide (ZrO_xH_y) aerogels as substrates for the sorption and degradation of the common organophosphorus simulant, DMMP (Long et al., 2020). Zirconia gels are synthesized via reaction of propylene oxide with aqueous solutions of $ZrCl_4$, ultimately yielding fragile aerogel monoliths after supercritical drying. Further heat treatment at temperatures ≥350°C removes residual organic contaminants derived from the epoxide-based synthesis and activates the zirconia aerogel toward the sorption and degradation of vapor-phase DMMP.

In situ infrared spectroscopy of zirconia aerogel powders verifies partial hydrolysis and degradation of DMMP, generating zirconium–methoxy fragments (Zr–OCH_3) on the

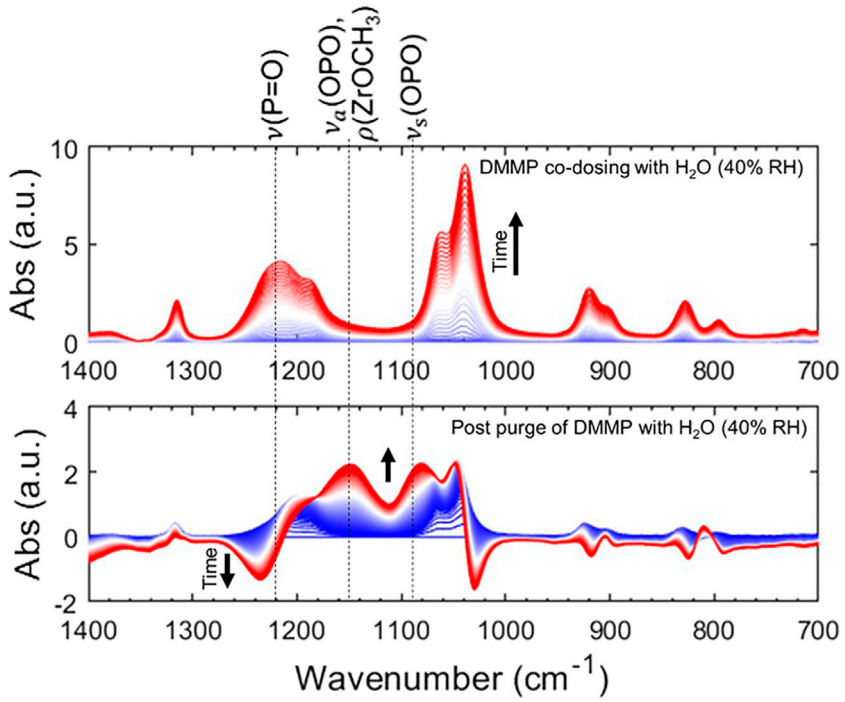

FIGURE 7 | Time-resolved attenuated total reflection–infrared spectroscopy (ATR-IR) of ZrO_xH_y aerogels under DMMP dosing **(top)** and DMMP removal **(bottom)**. Adapted from Long et al. (2020) with permission from the American Chemical Society.

ZrO_xH_y surface. Aerogel-expressed ZrO_xH_y maintains and even enhances reactivity with DMMP in the presence of humidity, as shown in the dynamic IR spectra in **Figure 7** for exposure under 40% RH conditions. Much like $Zr(OH)_4$, zirconia aerogels are rich in surface hydroxyl groups that provide reactive sites for molecules such as DMMP. The ZrO_xH_y aerogels are less vigorously reactive toward DMMP when compared to $Zr(OH)_4$, a trait that may be advantageous in some circumstances. For example, ZrO_xH_y aerogels evolve less vapor-phase methanol (a moderately toxic molecule) from their sorption/decomposition of DMMP. They also exhibit greater thermal stability, with reactive hydroxyls persisting even after heating the aerogel as high as 600°C.

COMPOSITE OXIDE AEROGELS AND METAL-MODIFIED AEROGELS

As a starting point, oxide aerogels offer molecularly accessible high surface area and a high number density of distributed reactive sites (e.g., hydroxyl groups) to neutralize chemical threats. Aerogels can then be modified by impregnating with reactive compounds, compositing with other oxides, or supporting metal nanoparticles to incorporate enhanced degradative or catalytic activity. Aerogel synthetic routes provide design flexibility to incorporate additional functionality (**Figure 3**), thereby increasing decontamination efficacy (Rolison et al., 2002). For example, blending two or more oxides in a composite aerogel can exploit synergistic interactions between the oxides and thus improve degradation efficiency for a number of TICs. Composite aerogels have been prepared in core@shell-like configurations by depositing an oxide layer on an aerogel (Klabunde et al., 1996; Jiang et al., 1998; Carnes and Klabunde, 2002; Martyanov and Klabunde, 2004) or through a co-gelation route where multiple oxide precursors are incorporated into sol–gel synthesis (Carnes et al., 2002; Prasad et al., 2010; Vu et al., 2015). Analogous to activated carbon, impregnation with active compounds can improve the degradative capability of adsorptive oxides. By supporting metal nanoparticles in the aerogel, a heterojunction is created that can activate small molecules and promote degradation reactions.

Impregnating Al_2O_3 aerogels (Saxena et al., 2009; Saxena et al., 2010b) or coupling them with other oxides (Prasad et al., 2010) improves their performance for protection against 2-CEES (Saxena et al., 2009), DCP (Saxena et al., 2010b), sarin (Saxena et al., 2010b), and HD (Prasad et al., 2010). Saxena et al. postulate that the degradation efficiency of metal oxides can be enhanced by impregnating them with reactive compounds already proven to neutralize toxic agents (Saxena et al., 2009; Saxena et al., 2010b), similar to the approaches used for carbon. They performed kinetics studies of adsorption and degradation of sarin (Saxena et al., 2010b) and the simulants 2-CEES (Saxena et al., 2009) and DCP (Saxena et al., 2010b) at Al_2O_3 aerogels and Al_2O_3 aerogels impregnated with 9-molybdo-3-vanadophosphoric acid ($MoVPA(V_3)$), dodecatungsto-phosphoric acid (PTA), NaOH, or K_2OsO_4. All four of the impregnants reduce surface area and pore volume of Al_2O_3 by blocking meso/micropores

(Saxena et al., 2009; Saxena et al., 2010b). Unimpregnated Al_2O_3 has the highest adsorption capacity for all simulants and agents tested due to its higher surface area and more facile transport through its unoccluded pores, but the worst degradation capacity. The authors conclude that the best composition to remove 2-CEES is Al_2O_3 impregnated with MoVPA(V_3) because it yields modestly high equilibrium capacity combined with the most rapid equilibrium time (Saxena et al., 2009). Similarly, Al_2O_3 + MoVPA(V_3) aerogel is deemed to be the most effective system for removal of DCP and sarin when considering both physisorption and subsequent degradation (Saxena et al., 2010b).

Coupling Al_2O_3 with other oxides also enhances degradation activity. According to Prasad et al., the basic surface of Al_2O_3 is amenable to driving hydrolytic degradation of contaminants, but lacks enough Lewis acid and Brønsted acid sites to effectively drive the formation of other surface complexation products (Prasad et al., 2010). In order to blend Lewis acid, Brønsted acid, and additional basic sites, they form mixed metal–oxide aerogels by co-gelling Al_2O_3 sol with Fe_2O_3, V_2O_5, or CuO. Although the composites possess lower surface area and pore volume than pure Al_2O_3, all composite aerogels more rapidly degrade HD than the pure oxide aerogel (Prasad et al., 2010). Among the composites, Al_2O_3–V_2O_5 is the only one to drive HD degradation by combining hydrolysis, surface complexation, and oxidation (Prasad et al., 2010).

Comparing mesoporous Al_2O_3 to other oxides reveals that MgO may be a better oxide for compositing because MgO shows more promise for degradation of a suite of toxic compounds (Winter et al., 2009; Saxena et al., 2010a). Coating MgO and CaO with a layer of Fe_2O_3 increases degradation of CCl_4, SO_2, and H_2S relative to either oxide on its own (Klabunde et al., 1996; Carnes and Klabunde, 2002). The authors postulate that in these synergistic core@shell composites, iron chloride or iron sulfites/sulfides/oxysulfides form on the surface but are highly mobile in the Fe_2O_3 layer. These mobile species can then migrate to the oxide||oxide interface where they exchange ions with the core oxide (**Figure 8**). The formation of intermediate species and subsequent ion exchange are both thermodynamically favorable steps for the proposed reactions and oxide systems (Klabunde et al., 1996; Carnes and Klabunde, 2002).

The synergistic effects of other first-row transition metal–oxide shells coated on CaO and MgO were compared for a host of chlorocarbons as well as DMMP (Jiang et al., 1998). For V_2O_3 shells, like Fe_2O_3, solid-state ion exchange allows penetration into the underlying core, thereby regenerating an oxide-rich surface for additional catalytic activity. This regeneration of reactive surface oxide continues until complete conversion of the oxide core, thereby enhancing degradation capacity relative to the bare oxide (Jiang et al., 1998). The V_2O_3 layers promote conversion of the underlying oxides better than Fe_2O_3. In order to compare how universal this ion-exchange behavior is for different halogens in V_2O_3, the authors then investigated core@shell-like composites with MgO cores for removal of chlorofluorocarbons (CCl_3F) (Martyanov and Klabunde, 2004). After heat treatment, the two oxides react to form a MgV_xO_y phase. Similar to Fe_2O_3, the MgV_xO_y layer forms vanadium chloride that reacts with MgO, but the MgV_xO_y layer does not accumulate fluoride. The composites not only show higher activities for CCl_3F degradation compared to either bare oxide, but also shorten the induction period. Low weight loadings of vanadium shorten the induction period, but do not eliminate it (Martyanov and Klabunde, 2004).

In a different route to designing oxide composites, Carnes et al. synthesized Al_2O_3/MgO aerogels by blending aluminum and magnesium precursors in the sol–gel synthesis (Carnes et al., 2002). The MgO aerogel is the more active oxide for TIC degradation due to its more basic surface, but Al_2O_3 aerogels possess higher surface area (805 vs. 400 m^2g^{-1}). The co-gelled

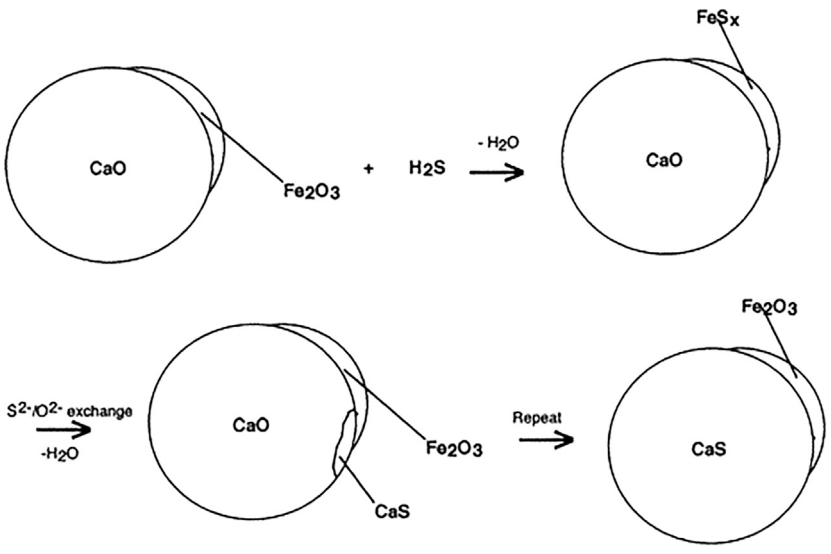

FIGURE 8 | Formation of intermediate species through ion exchange under H_2S adsorption in Fe_2O_3/CaO. Adapted from Carnes and Klabunde (2002) with permission from the American Chemical Society.

aerogel maintains—or even further improves upon—the surface reactivity of MgO while expressing MgO in a higher surface area form. The co-gelled aerogel with a 1:1 molar ratio of Al_2O_3/MgO takes on mesoscale characteristics more similar to the Al_2O_3 and possesses a surface area of 793 m^2g^{-1} (Carnes et al., 2002). These intermingled oxides enhance adsorption capacity and degradation capacity over either pure oxide aerogel for SO_2 and the CW simulant Paraoxon (Carnes et al., 2002). This enhanced capacity is due, in part, to forcing MgO into a higher surface-area phase, but also due to enhanced surface reactivity by promoting unusual morphologies and additional disorder (Carnes et al., 2002).

Vu et al. sought to improve upon the sorption capacity and reaction capacity of MgO by adding Fe_2O_3 or SiO_2 nanopowder to sol–gel precursors for MgO aerogels (Vu et al., 2015). The MgO + Fe_2O_3 composites have lower surface area and lower sorption capacity for 2-CEES but improved reactivity relative to MgO. In contrast, the MgO + SiO_2 mixtures have higher surface area and adsorption capacity for 2-CEES, but decreased reactivity relative to MgO. A MgO/SiO_2 composite aerogel synthesized through cogelation by adding silica precursors to the MgO precursors has smaller sorption capacities than the physical mixtures despite both composites containing 40 wt% SiO_2 (Vu et al., 2015). In the cogelled aerogels, SiO_2 covers the MgO particles, thus limiting access to the adsorptive/reactive MgO surface.

Contrasting two designs of composite aerogels—blending precursors vs. adding pre-formed solid guests to the sol (Vu et al., 2015) — highlights the fact that functionality is not derived from composition alone. The arrangement of solid-state components is also crucial for functionality. For example, when designing a composite that combines two or more phases (multiple metal oxides or metal + metal oxide), ensuring that sites at or near solid||solid interfaces are accessible is perhaps the single most important design consideration for optimal function. Rolison and co-workers coined the term "nanogluing" to describe the ability of about-to-gel sols to disperse a range of chemically and physically diverse guests into a host aerogel (Morris et al., 1999). Adding particulate guests—ranging from Pt nanoparticles, Au nanoparticles, Vulcan carbon, metal-oxide particles, and micron-sized zeolite crystallites—to silica sols just prior to gelation ensures that the guest is not fully enveloped by the oxide sol during gelation and that guest surfaces remain molecularly accessible (Morris et al., 1999; Rolison et al., 2002). Catalytic Au nanoparticles could be dispersed in a TiO_2 aerogel (Pietron et al., 2002) using a similar procedure. Adding mixed methyl + carboxy monolayer–protected Au nanoparticles to a titania sol prior to gelation yields a composite aerogel in which the Au nanoparticles have a uniform size distribution and are highly dispersed (Pietron et al., 2002). Their distribution is facilitated by initial adsorption at an amorphous, highly hydroxylated support with abundant nucleation sites. The resulting Au–TiO_2 guest–host composite shows remarkably high catalytic activity on the basis of Au loading, which arises from a high density of Au||TiO_2 interfaces with a high degree of contact intimacy augmented by an ability to size-stabilize the Au nanoparticles (Pietron et al., 2002; Pennington et al., 2020).

Although the majority of composite aerogels used for decontamination of CW agents and TICs discussed thus far are based on Al_2O_3 and MgO, other promising oxides have also been identified. In particular, TiO_2 is one of the most active and versatile oxides for remediation of CW simulants and other toxic compounds (Trubitsyn and Vorontsov, 2005; Panayotov and Morris, 2009a; Panayotov and Morris, 2009b; Winter et al., 2009). Additionally, highly reducible metal oxides such as TiO_2 and ceria (CeO_2) are less susceptible than other oxides to poisoning with adsorbed phosphorous compounds (Ratliff et al., 2009; Chen et al., 2010). These reducible oxides offer multiple adsorption/degradation cycles with DMMP prior to deactivation (Ratliff et al., 2009; Chen et al., 2010). Despite this promise, TiO_2 surfaces still mainly drive hydrolytic, stoichiometric degradation of organophosphorus compounds, although efforts underway seek to activate other degradation pathways and enhance active site turnover. Oxidative degradation pathways can be initiated, delaying deactivation by exciting the semiconducting bandgap of TiO_2 (Trubitsyn and Vorontsov, 2005; Sato et al., 2011; Hirakawa et al., 2013; Komano et al., 2013) or by creating metal||TiO_2 heterojunctions with supported metal nanoparticles (Panayotov and Morris, 2008; Ratliff et al., 2009). Gold nanoparticles supported on TiO_2 drive degradation of organophosphorus compounds, including complete oxidation of DMMP, by activating O_2 species at the Au||TiO_2 interface (O_2^-) (Panayotov and Morris, 2008). Exciting the TiO_2 bandgap during DMMP exposure simultaneously drives adsorption, hydrolysis, and photooxidation, resulting in faster removal of DMMP than occurs in the dark or under sequential dark/illuminated conditions (Trubitsyn and Vorontsov, 2005).

While TiO_2 performs as a reactive adsorbent (Trubitsyn and Vorontsov, 2005; Panayotov and Morris, 2009a; Panayotov and Morris, 2009b; Winter et al., 2009), a photocatalyst (Trubitsyn and Vorontsov, 2005; Sato et al., 2011; Hirakawa et al., 2013; Komano et al., 2013), and a metal support for degradation of CW agents (Panayotov and Morris, 2008; Ratliff et al., 2009), DeSario and co-workers developed composite TiO_2 aerogels that incorporate these multiple functions into a single platform. **Figure 9A** illustrates the synthesis of Cu/TiO_2 aerogels through photodeposition, with inset transmission electron micrographs showing the highly porous network structure. The TiO_2 aerogel provides a high surface area for CW agent adsorption, facilitates mass transport via the mesoporous network, and serves as a promoting support for catalytic/plasmonic nanoparticles of Cu (DeSario et al., 2017; DeSario et al., 2019; Maynes et al., 2020; McEntee et al., 2020; DeSario et al., 2021) or Au (DeSario et al., 2013; Panayotov et al., 2013; Pennington et al., 2020; Rolison et al., 2020). Coupling TiO_2 to supported metal nanoparticles provides the dual benefits of enhancing dark and photo-driven degradation pathways. The metal||oxide interface provides a reactive perimeter that activates molecular species, including H_2O and O_2, which initiate degradation of organophosphorous (OP) compounds. Choosing metals that possess a surface plasmon resonance (SPR) in the visible (e.g., Au, Cu) sensitizes the wide bandgap

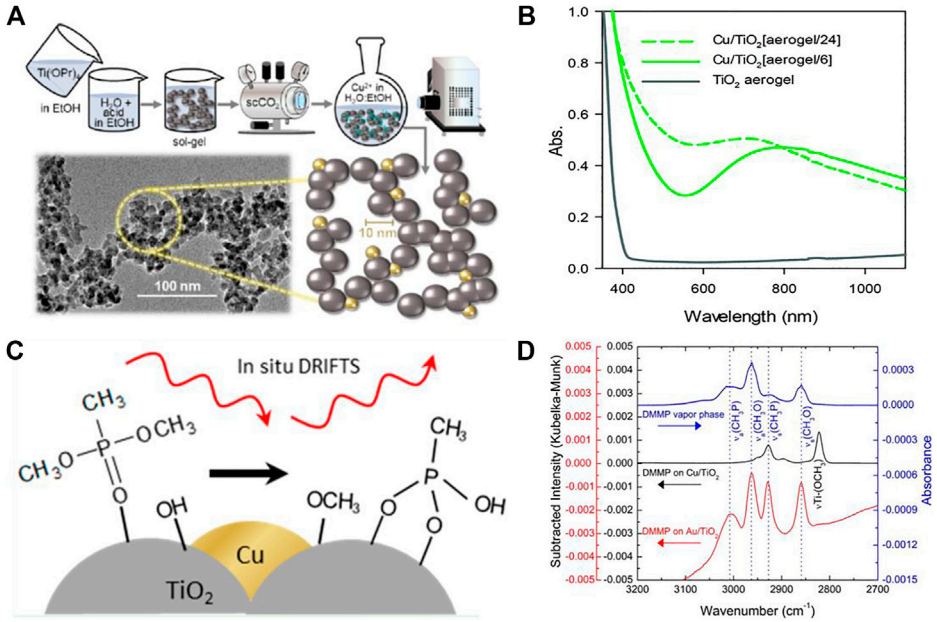

FIGURE 9 | (A) Synthetic schematic to prepare Cu/TiO_2 aerogels (inset: accompanying transmission electron micrograph of resulting composite aerogel). **(B)** UV–vis spectra for Cu NP-decorated and pristine TiO_2 aerogels. **(C)** Degradation pathway of DMMP over Cu/TiO_2 aerogels. **(D)** Spectrum of DMMP using diffuse reflectance infrared Fourier transform spectroscopy (DRIFTS) and DRIFTS difference spectra of DMMP-exposed Cu/TiO_2 and Au/TiO_2 aerogels. **(A**, **C**, and **D)** adapted from McEntee et al. (2020) with permission from the American Chemical Society. **(B)** adapted from DeSario et al. (2017) with permission from the Royal Society of Chemistry.

of TiO_2 into a broader portion of the solar spectrum (DeSario et al., 2013; DeSario et al., 2017), **Figure 9B**.

McEntee et al. characterized the hydrolytic degradation of DMMP on composite Cu/TiO_2 aerogels and Au/TiO_2 aerogels under aerobic and anaerobic conditions (McEntee et al., 2020). The Cu/TiO_2 aerogels prepared by photodepositing ~3–5 nm diameter Cu nanoparticles (DeSario et al., 2017; DeSario et al., 2019; Maynes et al., 2020) exhibit significantly faster and more complete hydrolytic degradation of DMMP compared to Au/TiO_2 or TiO_2 aerogels. After 1 h of exposure to DMMP vapor, only hydrolysis products are observed on the Cu/TiO_2 aerogel surface (McEntee et al., 2020). In the proposed mechanism, a surface-adsorbed OH group cleaves methoxy (CH_3O) groups of DMMP through nucleophilic attack, leaving methyl phosphonate on the surface (**Figure 9C**). In contrast, TiO_2 or Au/TiO_2 aerogels retain intact DMMP, as observed in the spectra obtained by diffuse-reflectance infrared Fourier transform spectroscopy (**Figure 9D**). The high hydrolytic activity of Cu/TiO_2 is attributed to a high surface concentration of basic OH groups that form at Cu||TiO_2 junctions, whereas these excess surface OH species are not observed to the same extent on Au/TiO_2 aerogels. Hydrolysis of DMMP is accelerated in the presence of O_2 due either to regeneration of active OH sites or promotion of oxidative pathways through O_2 activation at the metal||oxide junctions (McEntee et al., 2020).

DeSario et al. then demonstrated that the high hydrolytic activity of Cu/TiO_2 aerogels, combined with photoactivity courtesy of broadband excitation of the TiO_2 bandgap and Cu SPR, provides a powerful combination of hydrolysis + oxidation that enables rapid degradation of live chemical agents (DeSario et al., 2021). Sarin, like DMMP, degrades rapidly on the Cu/TiO_2 aerogel surface by hydrolytic routes by consuming basic, surface OH sites. Broadband illumination accelerates degradation of sarin with products more fully mineralized than in the dark. Under visible illumination (>480 nm), which excites the Cu SPR but not the TiO_2 bandgap, the rate of hydrolysis product accumulation is accelerated on Cu/TiO_2, while no additional degradation is driven on TiO_2 (DeSario et al., 2021).

At present, only a handful of reports describe SPR-initiated degradation of CW agents (Alvaro et al., 2010; Kuhn et al., 2019). These reports, as well as most of the plasmonic photocatalysis literature in general, utilize Ag or Au as the plasmonic sensitizer. In contrast, plasmonic applications for nonprecious and more abundant Cu are limited by its propensity to oxidize at the expense of its plasmon resonance. The intimate interfacial contact between photodeposited Cu nanoparticles and the TiO_2 aerogel stabilizes a high fraction of catalytically active Cu(0/I) and a sufficient amount of Cu(0) to maintain its plasmon resonance, unlike Cu nanoparticles photodeposited on larger, nanoparticulate TiO_2 supports (DeSario et al., 2017; DeSario et al., 2019; Maynes et al., 2020). Recent work with photodepositing Cu nanoparticles on ceria (CeO_2) aerogels finds retention of Cu plasmonic function and even higher catalytic activity for thermal oxidation of the model probe CO as compared to Cu/TiO_2 aerogel (Pitman, et al., 2020), pointing the way to another pore–solid oxide architecture with promise for the more challenging reactions necessary to remediate CW agents and TICs.

SUMMARY AND OUTLOOK

Recent research demonstrates the tremendous potential of various metal-oxide aerogels for protection against CW agents and TICs. While early work largely focused on the performance of unmodified metal-oxide aerogels, later design strategies reveal a wide variety of viable routes towards improving performance. Aerogels inherently arrange co-mapping of a high surface-area solid network with a highly mesoporous network to ensure facile transport of the chosen molecule to active sites dispersed throughout the structure. From this starting point, surfaces can be optimized through metal impregnation to induce additional acid/base sites, or treated to tune the oxide/hydroxide phase, with these approaches improving adsorptive and/or degradative properties. Native oxide aerogels have been heteroatom doped to increase oxygen vacancy content or doped with high-valent cations to impart proton-stabilized cation vacancies that increase the number density of lattice hydroxyls. Introducing heterojunctions by incorporating guests during or after gelation can further promote OH content throughout the entire oxide network. Decoration with metallic NPs such as Cu or Au can also benefit aerogels by activating H_2O or O_2 at the metal||oxide interface beyond that inherent to the oxide network alone as well as serving as plasmonic sensitizers to promote photocatalysis.

We expect future development of aerogel-based protective materials to benefit from better identification and optimization of specific active species, particularly by tailoring surface chemistry (oxide/hydroxide phases) and metal NP speciation. In particular, heteroatom doping in oxides to tune oxygen vacancy concentration is known to impart significant electronic effects (Laberty-Robert et al., 2007), but remains unexplored in this application space. Recent insights into the importance of the metal||oxide junction morphology for mesoscale electrical transport (Rolison et al., 2020) indicate that optimization of NP morphology on oxide aerogels could reap further benefits.

In addition to progression on the materials design front, future research must also address the current gap between laboratory and field conditions. A key advantage of oxide aerogels in general is their ambient stability and capability to prevent pore flooding (Rolison et al., 2002; Doescher et al., 2005), but the effect of humidity on many of the more recently reported NP-decorated aerogels needs systematic study under field conditions. It also remains to be seen if complete turnover of adsorptive/reactive sites occurs for these reactions under long-term, continuous operating conditions. If extensive surface poisoning occurs, the development of regeneration techniques using some combination of light, heat, or chemical treatments will be necessary for practical utilization of these reactive sorbents.

AUTHOR CONTRIBUTIONS

All authors listed have made a substantial, direct, and intellectual contribution to the work and approved it for publication.

FUNDING

This work was supported by the Defense Threat Reduction Agency (contract RD-CBT-PS1BR-CB10992 and RD-CBT-PS1BR-10300), the Office of Naval Research, and an NRL-National Research Council Postdoctoral Fellowship.

REFERENCES

Ahmed, E., Khanderi, J., Anjum, D. H., and Rothenberger, A. (2014). Selective Adsorption of Volatile Hydrocarbons and Gases in High Surface Area Chalcogels Containing $[ES_3]^{3-}$ Anions (E = As, Sb). *Chem. Mater.* 26, 6454–6460. doi:10.1021/cm502942w

Ahn, C., Park, J., Kim, D., and Jeon, S. (2013). Monolithic 3D Titania with Ultrathin Nanoshell Structures for Enhanced Photocatalytic Activity and Recyclability. *Nanoscale* 5, 10384–10389. doi:10.1039/C3NR03115B

Alvaro, M., Cojocaru, B., Ismail, A. A., Petrea, N., Ferrer, B., Harraz, F. A., et al. (2010). Visible-light Photocatalytic Activity of Gold Nanoparticles Supported on Template-Synthesized Mesoporous Titania for the Decontamination of the Chemical Warfare Agent Soman. *Appl. Catal. B: Environ.* 99, 191–197. doi:10.1016/j.apcatb.2010.06.019

Bandosz, T. J., Laskoski, M., Mahle, J., Mogilevsky, G., Peterson, G. W., Rossin, J. A., et al. (2012). Reactions of VX, GD, and HD with Zr(OH)4: Near Instantaneous Decontamination of VX. *J. Phys. Chem. C* 116, 11606–11614. doi:10.1021/jp3028879

Brinkert, K., Richter, M. H., Akay, Ö., Giersig, M., Fountaine, K. T., and Lewerenz, H.-J. (2018). Advancing Semiconductor-Electrocatalyst Systems: Application of Surface Transformation Films and Nanosphere Lithography. *Faraday Discuss.* 208, 523–535. doi:10.1039/C8FD00003D

Canivet, J., Fateeva, A., Guo, Y., Coasne, B., and Farrusseng, D. (2014). Water Adsorption in MOFs: Fundamentals and Applications. *Chem. Soc. Rev.* 43, 5594–5617. doi:10.1039/C4CS00078A

Carnes, C. L., Kapoor, P. N., Klabunde, K. J., and Bonevich, J. (2002). Synthesis, Characterization, and Adsorption Studies of Nanocrystalline Aluminum Oxide and a Bimetallic Nanocrystalline Aluminum Oxide/Magnesium Oxide. *Chem. Mater.* 14, 2922–2929. doi:10.1021/cm011590i

Carnes, C. L., and Klabunde, K. J. (2002). Unique Chemical Reactivities of Nanocrystalline Metal Oxides toward Hydrogen Sulfide. *Chem. Mater.* 14, 1806–1811. doi:10.1021/cm011588r

Cavka, J. H., Jakobsen, S., Olsbye, U., Guillou, N., Lamberti, C., Bordiga, S., et al. (2008). A New Zirconium Inorganic Building Brick Forming Metal Organic Frameworks with Exceptional Stability. *J. Am. Chem. Soc.* 130, 13850–13851. doi:10.1021/ja8057953

Chen, D. A., Ratliff, J. S., Hu, X., Gordon, W. O., Senanayake, S. D., and Mullins, D. R. (2010). Dimethyl Methylphosphonate Decomposition on Fully Oxidized and Partially Reduced Ceria Thin Films. *Surf. Sci.* 604, 574–587. doi:10.1016/j.susc.2009.12.028

Chen, Y., Zhang, X., Mian, M. R., Son, F. A., Zhang, K., Cao, R., et al. (2020). Structural Diversity of Zirconium Metal-Organic Frameworks and Effect on Adsorption of Toxic Chemicals. *J. Am. Chem. Soc.* 142, 21428–21438. doi:10.1021/jacs.0c10400

Contreras, A. M., Yan, X.-M., Kwon, S., Bokor, J., and Somorjai, G. A. (2006). Catalytic CO Oxidation Reaction Studies on Lithographically Fabricated Platinum Nanowire Arrays with Different Oxide Supports. *Catal. Lett.* 111, 5–13. doi:10.1007/s10562-006-0123-x

Davis, M. E., and Lobo, R. F. (1992). Zeolite and Molecular Sieve Synthesis. *Chem. Mater.* 4, 756–768. doi:10.1021/cm00022a005

DeCoste, J. B., Browe, M. A., Wagner, G. W., Rossin, J. A., and Peterson, G. W. (2015). Removal of Chlorine Gas by an Amine Functionalized Metal-Organic Framework via Electrophilic Aromatic Substitution. *Chem. Commun.* 51, 12474–12477. doi:10.1039/C5CC03780H

DeCoste, J. B., and Peterson, G. W. (2014). Metal-Organic Frameworks for Air Purification of Toxic Chemicals. *Chem. Rev.* 114, 5695–5727. doi:10.1021/cr4006473

DeSario, P. A., Gordon, W. O., Balboa, A., Pennington, A. M., Pitman, C. L., McEntee, M., et al. (2021). Photoenhanced Degradation of Sarin at Cu/TiO_2 Composite Aerogels: Roles of Bandgap Excitation and Surface Plasmon Excitation. *ACS Appl. Mater. Inter.* 13, 12550–12561. doi:10.1021/acsami.0c21988

DeSario, P. A., Pietron, J. J., Brintlinger, T. H., McEntee, M., Parker, J. F., Baturina, O., et al. (2017). Oxidation-stable Plasmonic Copper Nanoparticles in Photocatalytic TiO_2 Nanoarchitectures. *Nanoscale* 9, 11720–11729. doi:10.1039/c7nr04805j

DeSario, P. A., Pietron, J. J., DeVantier, D. E., Brintlinger, T. H., Stroud, R. M., and Rolison, D. R. (2013). Plasmonic Enhancement of Visible-Light Water Splitting with $Au–TiO_2$ Composite Aerogels. *Nanoscale* 5, 8073–8083. doi:10.1039/c3nr01429k

DeSario, P. A., Pitman, C. L., Delia, D. J., Driscoll, D. M., Maynes, A. J., Morris, J. R., et al. (2019). Low-temperature CO Oxidation at Persistent Low-Valent Cu Nanoparticles on TiO_2 Aerogels. *Appl. Catal. B: Environ.* 252, 205–213. doi:10.1016/j.apcatb.2019.03.073

Dey, S., and Praveen Kumar, V. V. (2020). The Performance of Highly Active Manganese Oxide Catalysts for Ambient Conditions Carbon Monoxide Oxidation. *Curr. Res. Green Sustain. Chem.* 3, 100012. doi:10.1016/j.crgsc.2020.100012

Doescher, M. S., Pietron, J. J., Dening, B. M., Long, J. W., Rhodes, C. P., Edmondson, C. A., et al. (2005). Using an Oxide Nanoarchitecture to Make or Break a Proton Wire. *Anal. Chem.* 77, 7924–7932. doi:10.1021/ac051168b

Gan, G., Li, X., Fan, S., Wang, L., Qin, M., Yin, Z., et al. (2019). Carbon Aerogels for Environmental Clean-Up. *Eur. J. Inorg. Chem.* 2019, 3126–3141. doi:10.1002/ejic.201801512

Han, Q., Yang, L., Liang, Q., and Ding, M. (2017). Three-dimensional Hierarchical Porous Graphene Aerogel for Efficient Adsorption and Preconcentration of Chemical Warfare Agents. *Carbon* 122, 556–563. doi:10.1016/j.carbon.2017.05.031

Hasanpour, M., and Hatami, M. (2020). Photocatalytic Performance of Aerogels for Organic Dyes Removal from Wastewaters: Review Study. *J. Mol. Liquids* 309, 113094. doi:10.1016/j.molliq.2020.113094

Hirakawa, T., Sato, K., Komano, A., Kishi, S., Nishimoto, C. K., Mera, N., et al. (2013). Specific Properties on TiO_2 Photocatalysis to Decompose Isopropyl Methylphosphonofluoridate and Dimethyl Methylphosphonate in Gas Phase. *J. Photochem. Photobiol. A: Chem.* 264, 12–17. doi:10.1016/j.jphotochem.2013.04.012

Islamoglu, T., Chen, Z., Wasson, M. C., Buru, C. T., Kirlikovali, K. O., Afrin, U., et al. (2020). Metal-Organic Frameworks against Toxic Chemicals. *Chem. Rev.* 120, 8130–8160. doi:10.1021/acs.chemrev.9b00828

Itoh, H., Utamapanya, S., Stark, J. V., Klabunde, K. J., and Schlup, J. R. (1993). Nanoscale Metal Oxide Particles as Chemical Reagents. Intrinsic Effects of Particle Size on Hydroxyl Content and on Reactivity and Acid/Base Properties of Ultrafine Magnesium Oxide. *Chem. Mater.* 5, 71–77. doi:10.1021/cm00025a015

Jasuja, H., Peterson, G. W., Decoste, J. B., Browe, M. A., and Walton, K. S. (2015). Evaluation of MOFs for Air Purification and Air Quality Control Applications: Ammonia Removal from Air. *Chem. Eng. Sci.* 124, 118–124. doi:10.1016/j.ces.2014.08.050

Jiang, Y., Decker, S., Mohs, C., and Klabunde, K. J. (1998). Catalytic Solid State Reactions on the Surface of Nanoscale Metal Oxide Particles. *J. Catal.* 180, 24–35. doi:10.1006/jcat.1998.2257

Khan, N. A., Hasan, Z., and Jhung, S. H. (2013). Adsorptive Removal of Hazardous Materials Using Metal-Organic Frameworks (MOFs): A Review. *J. Hazard. Mater.* 244-245, 444–456. doi:10.1016/j.jhazmat.2012.11.011

Kim, K., Tiwari, A. P., Hyun, G., Novak, T. G., and Jeon, S. (2019). Improving Electrochemical Active Area of MoS_2 via Attached on 3D-Ordered Structures for Hydrogen Evolution Reaction. *Int. J. Hydrogen Energ.* 44, 28143–28150. doi:10.1016/j.ijhydene.2019.09.071

Kistler, S. S. (1931). Coherent Expanded Aerogels and Jellies. *Nature* 127, 741. doi:10.1038/127741a0

Klabunde, K. J., Stark, J., Koper, O., Mohs, C., Park, D. G., Decker, S., et al. (1996). Nanocrystals as Stoichiometric Reagents with Unique Surface Chemistry. *J. Phys. Chem.* 100, 12142–12153. doi:10.1021/jp960224x

Komano, A., Hirakawa, T., Sato, K., Kishi, S., Nishimoto, C. K., Mera, N., et al. (2013). Titanium Dioxide Photocatalytic Decomposition of Ethyl-S-Dimethylaminoethyl Methylphosphonothiolate (VX) in Aqueous Phase. *Appl. Catal. B: Environ.* 134-135, 19–25. doi:10.1016/j.apcatb.2012.12.036

Koper, O. B., Lagadic, I., Volodin, A., and Klabunde, K. J. (1997). Alkaline-earth Oxide Nanoparticles Obtained by Aerogel Methods. Characterization and Rational for Unexpectedly High Surface Chemical Reactivities. *Chem. Mater.* 9, 2468–2480. doi:10.1021/cm970357a

Koper, O., Li, Y. X., and Klabunde, K. J. (1993). Destructive Adsorption of Chlorinated Hydrocarbons on Ultrafine (Nanoscale) Particles of Calcium Oxide. *Chem. Mater.* 5, 500–505. doi:10.1021/cm00028a017

Kuhn, D. L., Zander, Z., Kulisiewicz, A. M., Debow, S. M., Haffey, C., Fang, H., et al. (2019). Fabrication of Anisotropic Silver Nanoplatelets on the Surface of TiO_2 Fibers for Enhanced Photocatalysis of a Chemical Warfare Agent Simulant, Methyl Paraoxon. *J. Phys. Chem. C* 123, 19579–19587. doi:10.1021/acs.jpcc.9b04026

Laberty-Robert, C., Long, J. W., Pettigrew, K. A., Stroud, R. M., and Rolison, D. R. (2007). Ionic Nanowires at 600 °C: Using Nanoarchitecture to Optimize Electrical Transport in Nanocrystalline Gadolinium-Doped Ceria. *Adv. Mater.* 19, 1734–1739. doi:10.1002/adma.200601840

Lee, J.-H., and Park, S.-J. (2020). Recent Advances in Preparations and Applications of Carbon Aerogels: A Review. *Carbon* 163, 1–18. doi:10.1016/j.carbon.2020.02.073

Lee, S. W., Lee, C., Goddeti, K. C., Kim, S. M., and Park, J. Y. (2017). Surface Plasmon-Driven Catalytic Reactions on a Patterned Co_3O_4/Au Inverse Catalyst. *RSC Adv.* 7, 56073–56080. doi:10.1039/C7RA10450B

Li, K., Rothfus, R. R., and Adey, A. H. (1968). Effect of Macroscopic Properties of Manganese Oxides on Absorption of Sulfur Dioxide. *Environ. Sci. Technol.* 2, 619–621. doi:10.1021/es60020a001

Livage, J., and Sanchez, C. (1992). Sol-gel Chemistry. *J. Non-Crystalline Sol.* 145, 11–19. doi:10.1016/S0022-3093(05)80422-3

Long, J. W., Chervin, C. N., Balow, R. B., Jeon, S., Miller, J. B., Helms, M. E., et al. (2020). Zirconia-based Aerogels for Sorption and Degradation of Dimethyl Methylphosphonate. *Ind. Eng. Chem. Res.* 59, 19584–19592. doi:10.1021/acs.iecr.0c02983

Long, J. W., and Rolison, D. R. (2007). Architectural Design, Interior Decoration, and Three-Dimensional Plumbing en Route to Multifunctional Nanoarchitectures. *Acc. Chem. Res.* 40, 854–862. doi:10.1021/ar6000445

Long, J. W., Stroud, R. M., and Rolison, D. R. (2001). Controlling the Pore–Solid Architecture of Mesoporous, High Surface Area Manganese Oxides with the Birnessite Structure. *J. Non-Crystalline Sol.* 285, 288–294. doi:10.1016/S0022-3093(01)00469-0

Long, J. W., Wallace, J. M., Peterson, G. W., and Huynh, K. (2016). Manganese Oxide Nanoarchitectures as Broad-Spectrum Sorbents for Toxic Gases. *ACS Appl. Mater. Inter.* 8, 1184–1193. doi:10.1021/acsami.5b09508

Maleki, H. (2016). Recent Advances in Aerogels for Environmental Remediation Applications: A Review. *Chem. Eng. J.* 300, 98–118. doi:10.1016/j.cej.2016.04.098

Martínez-Ahumada, E., López-Olvera, A., Jancik, V., Sánchez-Bautista, J. E., González-Zamora, E., Martis, V., et al. (2020). MOF Materials for the Capture of Highly Toxic H_2S and SO_2. *Organometallics* 39, 883–915. doi:10.1021/acs.organomet.9b00735

Martyanov, I. N., and Klabunde, K. J. (2004). Decomposition of CCl_3F over Vanadium Oxides and [MgVxOy]MgO Shell/core-like Particles. *J. Catal.* 224, 340–346. doi:10.1016/j.jcat.2004.02.026

Maynes, A. J., Driscoll, D. M., DeSario, P. A., Pietron, J. J., Pennington, A. M., Rolison, D. R., et al. (2020). Electronic Metal-Support Interactions in the Activation of CO Oxidation over a Cu/TiO_2 Aerogel Catalyst. *J. Phys. Chem. C* 124, 21491–21501. doi:10.1021/acs.jpcc.0c06026

McEntee, M., Gordon, W. O., Balboa, A., Delia, D. J., Pitman, C. L., Pennington, A. M., et al. (2020). Mesoporous Copper Nanoparticle/TiO_2 Aerogels for Room-Temperature Hydrolytic Decomposition of the Chemical Warfare Simulant Dimethyl Methylphosphonate. *ACS Appl. Nano Mater.* 3, 3503–3512. doi:10.1021/acsanm.0c00228

Meneses, J. M., Denoyel, R., and Rouquerol, J. (2008). "Removal of Low Vapour Pressure Toxic Substances by Nanoporous Materials," in *Nanoporous Materials* (World Scientific), 643–652.

Mohanan, J. L., Arachchige, I. U., Brook III, S. L., III, Ghosh, P., Liao, P., Bury, W., et al. (2005). Porous Semiconductor Chalcogenide Aerogels. *Science* 307, 397–400. doi:10.1126/science.1104226

Mondloch, J. E., Katz, M. J., Isley III, W. C., III, Ghosh, P., Liao, P., Bury, W., et al. (2015). Destruction of Chemical Warfare Agents Using Metal-Organic Frameworks. *Nat. Mater* 14, 512–516. doi:10.1038/nmat4238

Morris, C. A., Anderson, M. L., Stroud, R. M., Merzbacher, C. I., and Rolison, D. R. (1999). Silica Sol as a Nanoglue: Flexible Synthesis of Composite Aerogels. *Science* 284, 622–624. doi:10.1126/science.284.5414.622

Mukhopadhyay, S., Schoenitz, M., and Dreizin, E. L. (2020). Vapor-phase Decomposition of Dimethyl Methylphosphonate (DMMP), a Sarin Surrogate, in Presence of Metal Oxides. *Defence Tech.* doi:10.1016/j.dt.2020.08.010

Navrotsky, A. (2011). Nanoscale Effects on Thermodynamics and Phase Equilibria in Oxide Systems. *ChemPhysChem* 12, 2207–2215. doi:10.1002/cphc.201100129

Pajonk, G. M. (1994). "A Short History of the Preparation of Aerogels and Carbogels," in *Sol-Gel Processing and Applications*. Editor Y. A. Attia (Boston, MA: Springer US), 201–219. doi:10.1007/978-1-4615-2570-7_18

Panayotov, D. A., DeSario, P. A., Pietron, J. J., Brintlinger, T. H., Szymczak, L. C., Rolison, D. R., et al. (2013). Ultraviolet and Visible Photochemistry of Methanol at 3D Mesoporous Networks: TiO_2 and Au-TiO_2. *J. Phys. Chem. C* 117, 15035–15049. doi:10.1021/jp312583w

Panayotov, D. A., and Morris, J. R. (2008). Catalytic Degradation of a Chemical Warfare Agent Simulant: Reaction Mechanisms on TiO_2-Supported Au Nanoparticles. *J. Phys. Chem. C* 112, 7496–7502. doi:10.1021/jp7118668

Panayotov, D. A., and Morris, J. R. (2009a). Thermal Decomposition of a Chemical Warfare Agent Simulant (DMMP) on TiO_2: Adsorbate Reactions with Lattice Oxygen as Studied by Infrared Spectroscopy. *J. Phys. Chem. C* 113, 15684–15691. doi:10.1021/jp9036233

Panayotov, D. A., and Morris, J. R. (2009b). Uptake of a Chemical Warfare Agent Simulant (DMMP) on TiO_2: Reactive Adsorption and Active Site Poisoning. *Langmuir* 25, 3652–3658. doi:10.1021/la804018b

Pennington, A. M., Pitman, C. L., DeSario, P. A., Brintlinger, T. H., Jeon, S., Balow, R. B., et al. (2020). Photocatalytic CO Oxidation over Nanoparticulate Au-Modified TiO_2 Aerogels: The Importance of Size and Intimacy. *ACS Catal.* 10, 14834–14846. doi:10.1021/acscatal.0c03640

Peterson, G. W., DeCoste, J. B., Fatollahi-Fard, F., and Britt, D. K. (2014). Engineering UiO-66-NH_2 for Toxic Gas Removal. *Ind. Eng. Chem. Res.* 53, 701–707. doi:10.1021/ie403366d

Peterson, G. W., Karwacki, C. J., Feaver, W. B., and Rossin, J. A. (2009). Zirconium Hydroxide as a Reactive Substrate for the Removal of Sulfur Dioxide. *Ind. Eng. Chem. Res.* 48, 1694–1698. doi:10.1021/ie801403h

Peterson, G. W., and Rossin, J. A. (2012). Removal of Chlorine Gases from Streams of Air Using Reactive Zirconium Hydroxide Based Filtration Media. *Ind. Eng. Chem. Res.* 51, 2675–2681. doi:10.1021/ie200809r

Pierre, A. C., and Pajonk, G. M. (2002). Chemistry of Aerogels and Their Applications. *Chem. Rev.* 102, 4243–4266. doi:10.1021/cr0101306

Pietron, J. J., Stroud, R. M., and Rolison, D. R. (2002). Using Three Dimensions in Catalytic Mesoporous Nanoarchitectures. *Nano Lett.* 2, 545–549. doi:10.1021/nl025536s

Pitman, C. L., Pennington, A. M., Brintlinger, T. H., Barlow, D. E., Esparraguera, L. F., Stroud, R. M., et al. (2020). Stabilization of Reduced Copper on Ceria Aerogels for CO Oxidation. *Nanoscale Adv.* 2, 4547–4556. doi:10.1039/D0NA00594K

Prasad, G. K., Mahato, T. H., Pandey, P., Singh, B., Suryanarayana, M. V. S., Saxena, A., et al. (2007). Reactive Sorbent Based on Manganese Oxide Nanotubes and Nanosheets for the Decontamination of 2-Chloro-Ethyl Ethyl Sulphide. *Microporous Mesoporous Mater.* 106, 256–261. doi:10.1016/j.micromeso.2007.03.004

Prasad, G. K., Ramacharyulu, P. V. R. K., Batra, K., Singh, B., Srivastava, A. R., Ganesan, K., et al. (2010). Decontamination of Yperite Using Mesoporous Mixed Metal Oxide Nanocrystals. *J. Hazard. Mater.* 183, 847–852. doi:10.1016/j.jhazmat.2010.07.104

Qu, Y.-F., Guo, J.-X., Chu, Y.-H., Sun, M.-C., and Yin, H.-Q. (2013). The Influence of Mn Species on the SO_2 Removal of Mn-Based Activated Carbon Catalysts. *Appl. Surf. Sci.* 282, 425–431. doi:10.1016/j.apsusc.2013.05.146

Ratliff, J. S., Tenney, S. A., Hu, X., Conner, S. F., Ma, S., and Chen, D. A. (2009). Decomposition of Dimethyl Methylphosphonate on Pt, Au, and Au–Pt Clusters Supported on TiO_2(110). *Langmuir* 25, 216–225. doi:10.1021/la802361q

Rechberger, F., and Niederberger, M. (2017). Synthesis of Aerogels: From Molecular Routes to 3-Dimensional Nanoparticle Assembly. *Nanoscale Horiz.* 2, 6–30. doi:10.1039/C6NH00077K

Rolison, D. R. (2003). Catalytic Nanoarchitecture—The Importance of Nothing and the Unimportance of Periodicity. *Science* 299, 1698–1701. doi:10.1126/science.1082332

Rolison, D. R., Morris, C. A., Anderson, M. L., Swider Lyons, K. E., Merzbacher, C. I., Ryan, J. V., et al. (2002). *Mesoporous Composite Gels and Aerogels*. Washington, DC: US Patent 6492014.

Rolison, D. R., Pietron, J. J., Glaser, E. R., Brintlinger, T. H., Yesinowski, J. P., DeSario, P. A., et al. (2020). Power of Aerogel Platforms to Explore Mesoscale Transport in Catalysis. *ACS Appl. Mater. Inter.* 12, 41277–41287. doi:10.1021/acsami.0c10004

Sato, K., Hirakawa, T., Komano, A., Kishi, S., Nishimoto, C. K., Mera, N., et al. (2011). Titanium Dioxide Photocatalysis to Decompose Isopropyl Methylphosphonofluoridate (GB) in Gas Phase. *Appl. Catal. B: Environ.* 106, 316–322. doi:10.1016/j.apcatb.2011.05.032

Saxena, A., Mangal, H., Rai, P. K., Rawat, A. S., Kumar, V., and Datta, M. (2010a). Adsorption of Diethylchlorophosphate on Metal Oxide Nanoparticles under Static Conditions. *J. Hazard. Mater.* 180, 566–576. doi:10.1016/j.jhazmat.2010.04.071

Saxena, A., Sharma, A., Srivastava, A. K., Singh, B., Gutch, P. K., and Semwal, R. P. (2009). Kinetics of Adsorption of Sulfur Mustard on Al_2O_3 nanoparticles with and without Impregnants. *J. Chem. Technol. Biotechnol.* 84, 1860–1872. doi:10.1002/jctb.2258

Saxena, A., Srivastava, A. K., Singh, B., Gupta, A. K., Suryanarayana, M. V. S., and Pandey, P. (2010b). Kinetics of Adsorptive Removal of DEClP and GB on Impregnated Al_2O_3 Nanoparticles. *J. Hazard. Mater.* 175, 795–801. doi:10.1016/j.jhazmat.2009.10.078

Schwochow, F., and Puppe, L. (1975). Zeolites? Their Synthesis, Structure, and Applications. *Angew. Chem. Int. Ed. Engl.* 14, 620–628. doi:10.1002/anie.197506201

Shuvarakova, E. I., Bedilo, A. F., Chesnokov, V. V., and Kenzhin, R. M. (2018). Dehydrochlorination of 1-chlorobutane over Nanocrystalline MgO: The Role of Electron-Acceptor Sites. *Top. Catal.* 61, 2035–2041. doi:10.1007/s11244-018-1000-8

Smith, B. M. (2008). Catalytic Methods for the Destruction of Chemical Warfare Agents under Ambient Conditions. *Chem. Soc. Rev.* 37, 470–478. doi:10.1039/B705025A

Son, F. A., Wasson, M. C., Islamoglu, T., Chen, Z., Gong, X., Hanna, S. L., et al. (2020). Uncovering the Role of Metal-Organic Framework Topology on the Capture and Reactivity of Chemical Warfare Agents. *Chem. Mater.* 32 (11), 4609–4617. doi:10.1021/acs.chemmater.0c00986

Song, Y., Chau, J., Sirkar, K. K., Peterson, G. W., and Beuscher, U. (2020). Membrane-supported Metal Organic Framework Based Nanopacked Bed for Protection against Toxic Vapors and Gases. *Separat. Purif. Tech.* 251, 117406. doi:10.1016/j.seppur.2020.117406

Tang, H., Cheng, Z., Zhu, H., Zuo, G., and Zhang, M. (2008). Effect of Acid and Base Sites on the Degradation of Sulfur Mustard over Several Typical Oxides. *Appl. Catal. B: Environ.* 79, 323–333. doi:10.1016/j.apcatb.2007.10.036

Tenner, E. (1997). *Why Things Bite Back*. New York: Vintage. doi:10.21236/ada348473

Tiwari, A. P., Lee, K., Kim, K., Kim, J., Novak, T. G., and Jeon, S. (2020). Conformally Coated Nickel Phosphide on 3D, Ordered Nanoporous Nickel for Highly Active and Durable Hydrogen Evolution. *ACS Sustain. Chem. Eng.* 8, 17116–17123. doi:10.1021/acssuschemeng.0c05192

Trubitsyn, D. A., and Vorontsov, A. V. (2005). Experimental Study of Dimethyl Methylphosphonate Decomposition over Anatase TiO_2. *J. Phys. Chem. B* 109, 21884–21892. doi:10.1021/jp053793q

Vadjić, V., and Gentilizza, M. (1985). The Effect of MnO_2 and Some Manganese Salts on the Behaviour of Sulphur Dioxide in the Air Investigated on Model Systems. *Sci. Total Environ.* 44, 245–251. doi:10.1016/0048-9697(85)90098-1

Vu, A.-T., Jiang, S., Ho, K., Lee, J. B., and Lee, C.-H. (2015). Mesoporous Magnesium Oxide and its Composites: Preparation, Characterization, and Removal of 2-chloroethyl Ethyl Sulfide. *Chem. Eng. J.* 269, 82–93. doi:10.1016/j.cej.2015.01.089

Wagner, G. W., Bartram, P. W., Koper, O., and Klabunde, K. J. (1999). Reactions of VX, GD, and HD with Nanosize MgO. *J. Phys. Chem. B* 103, 3225–3228. doi:10.1021/jp984689u

Wagner, G. W., Koper, O. B., Lucas, E., Decker, S., and Klabunde, K. J. (2000). Reactions of VX, GD, and HD with Nanosize CaO: Autocatalytic Dehydrohalogenation of HD. *J. Phys. Chem. B* 104, 5118–5123. doi:10.1021/jp000101j

Wagner, G. W., Procell, L. R., O'Connor, R. J., Munavalli, S., Carnes, C. L., Kapoor, P. N., et al. (2001). Reactions of VX, GB, GD, and HD with Nanosize Al_2O_3. Formation of Aluminophosphonates. *J. Am. Chem. Soc.* 123, 1636–1644. doi:10.1021/ja003518b

Wang, G., Sharp, C., Plonka, A. M., Wang, Q., Frenkel, A. I., Guo, W., et al. (2017). Mechanism and Kinetics for Reaction of the Chemical Warfare Agent Simulant, DMMP(g), with Zirconium(IV) MOFs: An Ultrahigh-Vacuum and DFT Study. *J. Phys. Chem. C* 121, 11261–11272. doi:10.1021/acs.jpcc.7b00070

Wang, J., Liu, D., Li, Q., Chen, C., Chen, Z., Song, P., et al. (2019). Lightweight, Superelastic yet Thermoconductive Boron Nitride Nanocomposite Aerogel for Thermal Energy Regulation. *ACS Nano* 13, 7860–7870. doi:10.1021/acsnano.9b02182

Wang, J., Wang, X., and Zhang, X. (2017). Cyclic Molecule Aerogels: a Robust Cyclodextrin Monolith with Hierarchically Porous Structures for Removal of Micropollutants from Water. *J. Mater. Chem. A.* 5, 4308–4313. doi:10.1039/C6TA09677H

Wang, J., Zhang, P., Li, J., Jiang, C., Yunus, R., and Kim, J. (2015). Room-temperature Oxidation of Formaldehyde by Layered Manganese Oxide: Effect of Water. *Environ. Sci. Technol.* 49, 12372–12379. doi:10.1021/acs.est.5b02085

Wang, Z.-M., and Kanoh, H. (2001). Calorimetric Study on NH_3 Insertion Reaction into Microporous Manganese Oxides with (2×2) Tunnel and (2×∞) Layered Structures. *Thermochim. Acta* 379, 7–14. doi:10.1016/S0040-6031(01)00596-2

WangFang, H. Q., Fang, Q., Gu, W., Du, D., Lin, Y., and Zhu, C. (2020). Noble Metal Aerogels. *ACS Appl. Mater. Inter.* 12, 52234–52250. doi:10.1021/acsami.0c14007

Winter, M., Hamal, D., Yang, X., Kwen, H., Jones, D., Rajagopalan, S., et al. (2009). Defining Reactivity of Solid Sorbents: What Is the Most Appropriate Metric? *Chem. Mater.* 21, 2367–2374. doi:10.1021/cm8032884

Xie, P., Chen, Z., Xu, J., Xie, D., Wang, X., Cui, S., et al. (2019). Artificial Ceramic Diatoms with Multiscale Photonic Architectures via Nanoimprint Lithography for CO2 Photoreduction. *J. Am. Ceram. Soc.* 102, 4678–4687. doi:10.1111/jace.16334

Xu, R., Du, L., Adekoya, D., Zhang, G., Zhang, S., Sun, S., et al. (2020). Well-Defined Nanostructures for Electrochemical Energy Conversion and Storage. *Adv. Energ. Mater.* 11, 2001537. doi:10.1002/aenm.202001537

Yekta, S., Sadeghi, M., Mirzaei, D., Zabardasti, A., and Farhadi, S. (2019). Removal of Nerve Agent Sarin Simulant from Aqueous Solution Using the ZSM-5/$CoFe_2O_4$ NPs Adsorbent. *J. Iran. Chem. Soc.* 16, 269–282. doi:10.1007/s13738-018-1504-y

Zhang, L., Wang, S., Lv, L., Ding, Y., Tian, D., and Wang, S. (2021). Insights into the Reactive and Deactivation Mechanisms of Manganese Oxides for Ozone Elimination: The Roles of Surface Oxygen Species. *Langmuir* 37, 1410–1419. doi:10.1021/acs.langmuir.0c02841

Zhang, Y.-Z., El-Demellawi, J. K., Jiang, Q., Ge, G., Liang, H., Lee, K., et al. (2020). MXene Hydrogels: Fundamentals and Applications. *Chem. Soc. Rev.* 49, 7229–7251. doi:10.1039/D0CS00022A

Conflict of Interest: The authors declare that the research was conducted in the absence of any commercial or financial relationships that could be construed as a potential conflict of interest.